

# Design of an Integrated 100kW Permanent Magnet Synchronous Machine in a Prototype Thruster for Ship Propulsion

Ø. Krøvel, R. Nilssen, S. E. Skaar, E. Løvli<sup>1</sup>, N. Sandøy<sup>2</sup>

Department of Electrical Power Engineering, NTNU, Trondheim, Norway.

O.S. Bragstads plass 2E, 7491 Trondheim, Norway

Phone: +47 73594241 Fax: +47 73594279

Email: Oystein.Krovel@elkraft.ntnu.no

<sup>1</sup>SmartMotor AS, Trondheim, Norway

<sup>2</sup>Norpropeller AS, Molde, Norway

**Abstract:** -- Traditional electrical motors are mechanical coupled through gear and shaft to their load. This paper presents a direct driven permanent magnet (PM) motor integrated into a ship propeller. It is proven that an integration of PM-motor and propeller is possible. This design has better hydrodynamic properties than standard tunnel and azimuth thrusters. The electric machine is a surface mounted PM-machine with 22 poles and number of slots per pole per phase equal to 1.09.

## I. INTRODUCTION

Traditional thrusters on ship consist of a propeller, shaft, gear and a motor. Often the gear is placed directly behind the propeller, shaped as a bended knee with the shaft passing through the hull above the thruster. Fig 1 shows a traditional tunnel thruster with a knee gear (left). This design has some hydrodynamic drawbacks since the shaft and gear is in the path of the water. Vibrations can also be a problem since the shaft goes through the hull. An alternative solution is a rim driven thruster where the shaft and gear has been removed. There are only propeller blades in the water path and only electric cables go through the hull. This improves the efficiency of the propeller, removes the gear and reduces vibration. In this paper the design of an integrated electric machine is presented together with results from the testing of the electric machine. Bearings, hydrodynamics and noise are not discussed.

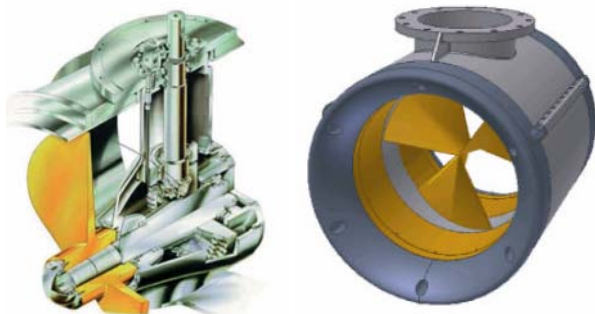


Fig 1, On the left is a traditional tunnel thruster from Rolls Royce [4]. On the right an azimuth thruster with integrated PM-machine

## II. INTEGRATION OF THE PERMANENT MAGNET MOTOR

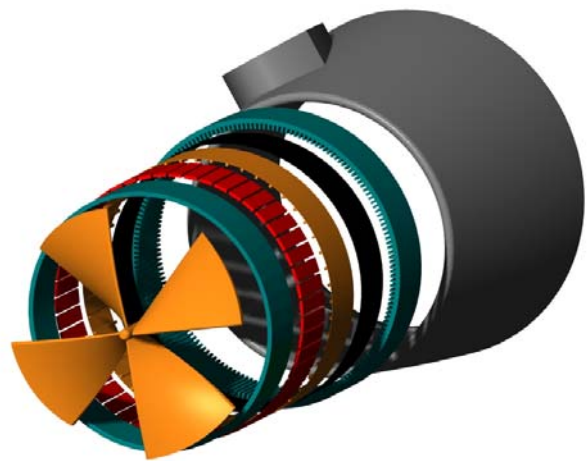


Fig 2, Exploded view of the integrated electric machine

The diameter, speed and power of the electrical machines are all design parameters which are given by the size and shape of the propeller blades i.e. hydrodynamics of the construction. For a given propeller design, the inner diameter of the hull (propeller diameter), the optimal speed and power are given. The space is also restricted; the motor is expected not to make the thruster, or nozzle, more voluminous. The motor is a part of a variable speed drive with inverter which makes the frequency a free variable. The voltage is also a relative free design parameter, but it is reasonable to adjust it to commonly used voltage levels on ships. The restrictions of dimensions, power and speed favours the PM-magnet machine with a relative high number of poles. Compared to conventional radial electrical machines, the relative large diameter and a high number of poles, result in a thin and short active machine.

### A. The PM-motor basics

Fig 2 gives an exploded view of the integrated PM-machine and Fig 3 is a sketch of the machine parts. The propellers are fixed to the inner side of the tunnel. The

tunnel is a ring made of soft iron and is magnetically the rotor yoke. The rotor yoke must therefore be dimensioned to account for both the magnetic flux and the mechanical forces from the propeller blades. A cage made of brass is fitted around the rotor yoke. The PM's are inserted into the cage and glued to the iron surface of the rotor yoke. The thruster has hydrodynamic bearings with water in the gap between the rotating and stationary parts. Since the magnets are highly corrosive they have to be covered. This is done by a band of fibre glass and epoxy coating. The stator with its copper and laminated core is covered by a tube made of non-magnetic, non-electric composite material. The stator is welded to an outer housing made of iron.

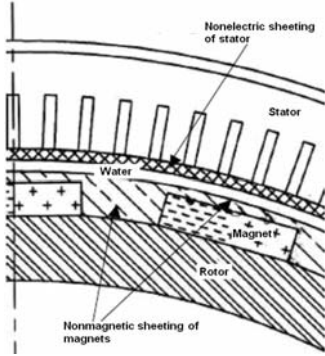


Fig 3, A sketch of the cross section of the machine with the different components

The gap and the shielding of rotor and stator add up to a relative large effective air gap.

### B. The Prototype Thruster

It was decided to build a 100kW prototype with an inner diameter of 600mm and a nominal speed of 700rpm. A line voltage of 400V was chosen, which gives a current of 150A. A compromise between frequency and pole pitch resulted in a pole number ( $N_p$ ) of 22 and a nominal frequency ( $f_n$ ) of 128Hz. The PM's are rectangular and mounted on the surface of the rotor yoke. The rotor yoke was chosen to be of solid soft iron. The stator lamination is 0.5mm thick. The magnets are neodym magnets (NdFeB) with a remanens ( $B_r$ ) of 1.2T.

To reduce the harmonics and to reduce the winding overhang a two layer fractional winding was chosen. The stator has 72 slots which results in a slot pr pole of  $36/11=3.27$  and a slot pr pole pr phase ( $q$ ) of  $12/11=1.09$ . Each coil spans 3 slots. This is a classic type of fractional winding [2]. In Table II some dimensions of the PM-machine are given.

## III. ELECTROMAGNETIC THEORY

The theory used for the calculations can be found in textbooks written by Hanselman [1] and Say [2]. Some basic functions and relations will be presented.

### A. Voltage

The voltage is found by the change in flux:

$$e_i = N \frac{d\phi}{dt} \quad (1)$$

The equation for the phase voltage is:

$$\begin{aligned} \hat{E} &= \sqrt{2} \cdot E_{rms} = k_d \cdot N_{sc} \cdot N \cdot \frac{d\phi}{dt} \\ &= 2 \cdot \pi \cdot k_d \cdot N_{sc} \cdot N \cdot \phi_{max} \cdot f \end{aligned} \quad (2)$$

Where  $N$  is number of turns,  $N_{sc}$  number of coils in series,  $k_d$  the distribution factor,  $\phi$  is the flux and  $f$  the frequency. It is assumed a sinusoidal flux wave. The flux is found from finite element calculations. If a lumped circuit equivalent is used to find the flux, the voltage must also be multiplied with the chording factor.

### B. Chording and distribution factor

The chording factor ( $k_p$ ) describes the voltage reduction when the coil does not enclose all flux lines from one pole. For the first harmonic the equation is:

$$k_p = \sin\left(\frac{\theta_{ce}}{2}\right) \quad (3)$$

Where  $\theta_{ce}$  is the coil span in electrical degrees.

The distribution factor takes into account that the voltages from the coils connected in series is not in phase. For the first harmonic the equation is:

$$k_d = \frac{\sum_{i=1}^{N_{sc}} \cos(\psi^i)}{N_{sc}} \quad (4)$$

Where  $\psi$  is the phase displacement for each coil. Both the distribution and chording of the windings affects the harmonics of voltage. If chosen correctly they can both strongly reduce troublesome harmonic without affecting the first harmonic to much.

### C. Inductance

The inductance is found by using the energy equations:

$$W = \frac{1}{2} Li^2 = \frac{1}{2} \int B \cdot HdV \quad (5)$$

Using finite element methods the energy can easily be calculated by integrating the energy density over the actual domains or area. The current applied is known, and the inductance can be found:

$$L = \frac{2 \cdot W}{I^2} \quad (6)$$

The inductance for the end windings has been neglected. For a distributed winding the mutual inductance can be assumed to be one third of the slot inductance, neglecting the chording. This leads to a total inductance pr phase:

$$L_{phase} = \frac{4 \cdot L_{coil}}{3} \cdot N_{sc} \quad (7)$$

#### D. Resistance

The resistance is calculated from an estimate of the copper length and area for each turn. The copper area is:

$$A_{Cu} = A_{eff} \cdot k_{Cu} = \left( A_{slot} - [A_{iso} + A_{wedge}] \right) \cdot k_{Cu} \quad (8)$$

$$A_{turn} = \frac{A_{Cu}}{N}$$

$A_{Cu}$  is the total copper area,  $A_{slot}$  the total slot area and  $A_{iso}$  and  $A_{wedge}$  the area occupied by respectively the slot insulation and the slot wedge. A drawing of the tooth geometry is added in the appendix (Fig 11).  $k_{Cu}$  is the copper fill factor. The length is:

$$l_{turn} = 2 \cdot L + 2 \cdot \frac{\tau_c}{2} \pi = 2 \cdot L + \tau_c \cdot \pi \quad (9)$$

Where  $L$  is the machine length and  $\tau_c$  the coil pitch ([m]). The resistance is:

$$R_a = \frac{N_{sc} \cdot N \cdot l_{turn}}{A_{turn} \cdot k_T \cdot \sigma_{Cu}} \quad (10)$$

$k_T$  is the temperature coefficient. It is expressed as [2]:

$$k_T = \frac{k + 20^\circ}{k + T_n} \quad (11)$$

where  $T_n$  is the temperature in the windings at nominal load and  $k$  is the resistant-temperature coefficient ( $k=234$ ).

#### E. Losses

The copper losses are:

$$P_{Cu} = I^2 R_a \quad (12)$$

The iron losses are dependent of the voltage and frequency. They can be derived from data provided by the manufacture of the sheet metal. The equations for iron losses are:

$$P_e = k_e \cdot f^2 \cdot B_{max}^2 \quad (13)$$

$$P_h = k_h \cdot f \cdot B_{max}^n$$

$P_e$  is the eddy current loss and  $P_h$  is the hysteresis loss

## IV. ANALYTIC CALCULATION

### A. Distribution and chording factor

Due to both the chording and distribution of the coils the sum of voltages will be slightly reduced compared to the scalar sum all coil voltages in series. The chording factor is:

$$k_p = \sin\left(\frac{180 \cdot (3 \cdot 22/72)}{2}\right) = 0.991 \quad (14)$$

The distribution factor is found by looking at the phase angels between the induced voltages in the different coils connected in series.  $q$  is equal to 12/11. This means that for every 11<sup>th</sup> pole the machine repeats it self magnetically. And for this machine, only half of the machine has to be considered since there are 22 poles. For one half of the machine there are 12 coils in series pr phase. Table I shows the phase angles relative to coil nr 1.

TABLE I  
PHASE ANGLE BETWEEN COILS CONNECTED IN SERIES

Coil nr	Phase displacement (el°)	corrected for neutral point: 27.5° (el°)
1	0	27.5
2	55	-27.5
3	40	-12.5
4	25	+2.5
5	10	+17.5
6	50	-22.5
7	35	-7.5
8	20	+7.5
9	5	+22.5
10	45	-17.5
11	30	-2.5
12	10	+12.5

Considering the phase angles corrected for the neutral point and the equation for the distribution factor, it is found that the winding is symmetric and only 6 coils has to be considered. The distribution factor for the first harmonic is:

$$k_d = 0.955 \quad (15)$$

### B. Losses

The losses in the machine will be copper losses and iron losses. The resistance is:

$$R_a = \frac{24 \cdot 3 \cdot 628}{32.5 \cdot 0.7 \cdot 58 \cdot 10^6} = 0.0343 \Omega \quad (16)$$

It is assumed high temperature (130°) at nominal load (a conservative choice). At nominal load (100kW) the copper loss is  $P_{Cu} = 2380W$ . By extrapolating the data for iron losses in the sheet metal, the losses in the stator are found to be  $P_{st} = 388W$  at 128 Hz. This gives a total loss of  $P_{loss} = 2800W$  and an expected efficiency of 0.97. It should be mentioned that this is a very optimistic efficiency. Losses in rotor yoke, magnets, brass and housing are not included.

## V. FINITE ELEMENT ANALYSIS

Finite Element analyses were used to calculate the flux (voltage) and inductance. It was also used to observe the flux distribution in the machine. For the calculations of the flux density in the iron a saturation curve was used. This curve was an interpolation of data obtained from the suppliers of sheet metal.

The maximum flux going through one coil is found to be 0.0054Wb. Using (2), the voltage is found:

$$\begin{aligned}\hat{E} &= \sqrt{2} \cdot E_{rms} = 2 \cdot \pi \cdot k_d \cdot N_{sc} \cdot N \cdot \phi_{max} \cdot f \\ &= 2 \cdot 0.955 \cdot 24 \cdot 3 \cdot 0.0054 \cdot 128 = 311V \\ E_{rms} &= 220V\end{aligned}\quad (17)$$

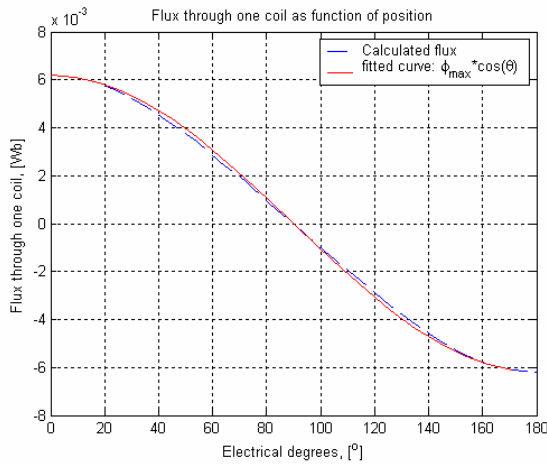


Fig 4, The change of flux when rotating the rotor 180 electrical degrees

Fig 4 shows the change of the flux through one coil when the rotor is rotated 180 electrical degrees. This verifies the assumption that the flux wave has a sinusoidal shape, and thereby also the voltage will be a sinusoidal. Fig 5 shows the flux lines and flux densities for two poles.

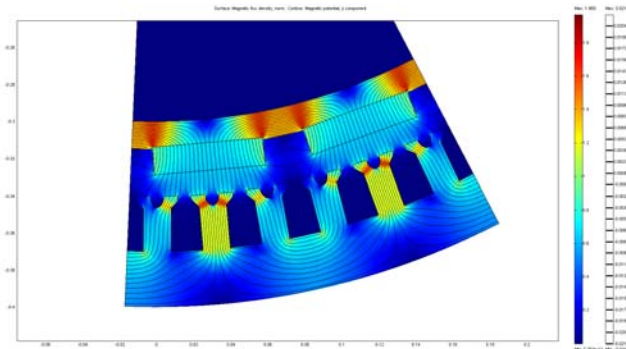


Fig 5, A 2D-plot of the flux density and flux lines for two poles.

The inductance is calculated from the energy stored in the machine when current is applied. The energy stored in two coils is calculated to 0.48J. From (6) the inductances for one phase is calculated to  $L_{phase}=0.477mH$ . At 128Hz this represent at reactance of  $0.384\Omega$  or  $0.27pu$ .

## VI. TESTING

The thruster has been tested both onshore as a generator, Fig 6, and also mounted on a boat for testing, Fig 7.

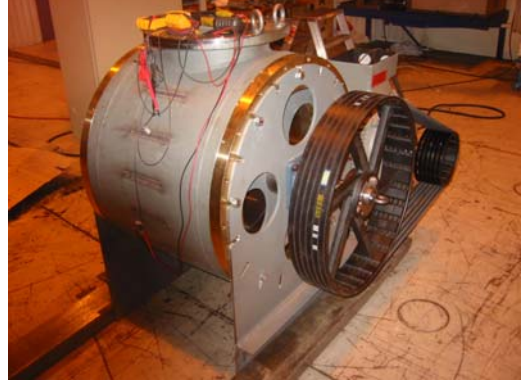


Fig 6, Generator tests onshore in Brunvoll AS' premises



Fig 7, The boat used for testing. The thruster is in front of the picture, not yet mounted.

### A. Generator test

The machine was tested as a generator onshore. As expected the voltage is proportional to the speed, it is 0.573V/rpm. It is found that the induced line voltage at 700rpm is 401V, which is slightly higher than the calculated value. Fig 8 shows a photo of the three phases at a low speed (about 40 rpm).

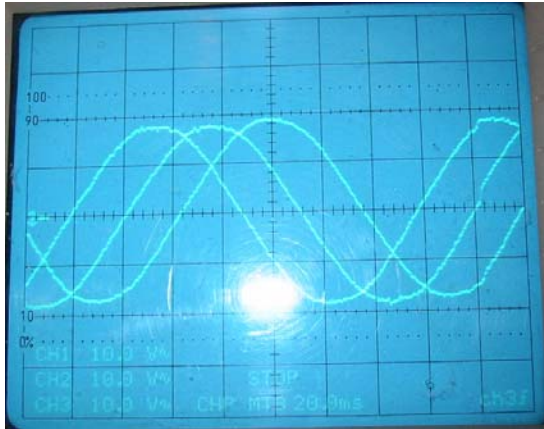


Fig 8, Picture of the voltage of the three phases. One of the phases is inverted for the occasion.

The efficiency of the machine was also tested onshore. The measurement of input power (torque and speed) was strongly affected by noise, and therefore the measurements are somewhat inaccurate. The efficiency is plotted for different speeds in Fig 9. The mean efficiency is approximated to 0.93. This is much lower than the calculated 0.97.

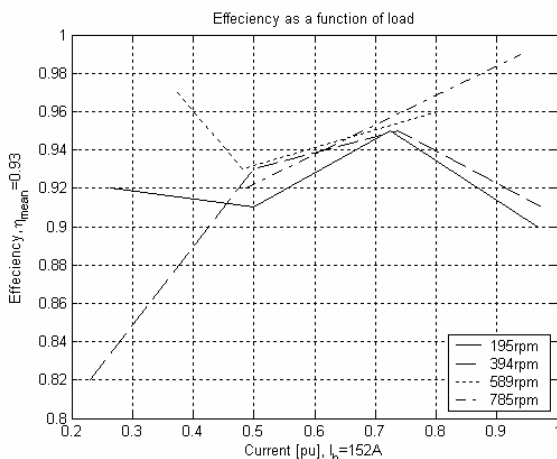


Fig 9, Plot of efficiency as a function of load

### B. Testing of the thruster mounted on the ship

Since this is an integrated machine in a thruster a summary of the towing test is presented. The temperatures in the machines were measured while the machines was submerged and working in the sea.

#### 1) Temperature measurement

The temperature was measured in the windings for different loads. It was found that the temperature rise was no more than 40°C at full load. Fig 10 shows the measured temperature for different loads. The measurements were done with the thruster submerged in the sea with an ambient temperature of 20°C.

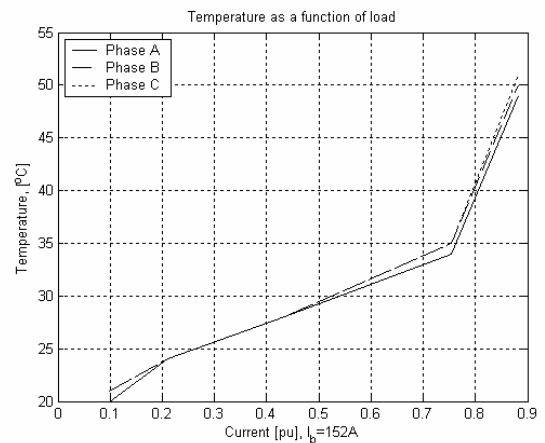


Fig 10 Temperature at different loads.

#### 2) Towing test

To test the thruster's capability to push and pull a towing test was conducted. This test is mainly depending on hydrodynamics of the propellers and other structure, and not so much of the electric machine. It proved that the thruster is as good as other tunnel and azimuth thrusters. It has twice the pull pr power (kg/kW) as conventional ideal open propeller. Since this is merely a prototype the potential for optimization of the structure is large.

## VII. DISCUSSION

The calculations gave good indications of voltage and load capability. The machine is a relative conservative construction. The design of the teeth was considered thoroughly. The teeth were designed to, from the magnets, look like a uniform surface. This to prevent cogging and torque ripple and eddy currents in the magnets. It also should be mentioned that with the chosen pole pitch, the number of slots pr pole and the relative large air gap, the rotor would not experience much changes in the reluctance during a rotation regardless off the shape of the teeth.

As the measurements shows, the losses are higher than expected. The measured efficiency is approximately 0.93. Several loss mechanisms, which are normally small, were not included in the total loss. These are losses in the rotor, stray load losses and mechanical losses. The brass cage surrounding the magnets gives possible higher rotor losses than expected. The winding overhang directly rest against the iron housing of the thruster. The proximity is likely to result in increased losses in the iron housing. In addition the winding overhang is larger than calculated (longer coils).

Because of the semi closed slots each coil had to be manually inserted. The thickest conductor which the coil manufacturer used was 1.4mm in diameter. This means that each coil consists of 3 turns with 21 parallel conductors short circuited for each turn, generating very good conditions for circulating currents.

Losses lead to higher temperatures. For this integrated machine cooling is not a problem. Water is constantly flowing through the rotor, the air gap (water gap) and around the stator. The measured temperature rise at full load, tested with the boat pulling at its mooring, does indicate that even though the losses are high, the temperatures are still well within their limits.

### VIII. CONCLUSION

It has been shown that it is possible to integrate a radial flux permanent magnet machine within an azimuth thruster. This combination gives a better hydrodynamic efficiency of the thruster and also removes the gear which is often used when applying medium speed inverter fed induction motors. During the design of the stator great care has been taken to avoid fluctuations of the flux in the rotor. The measured losses differ significantly from the calculated losses. The difference is most likely not caused by the simplification done in the calculations, but a result of losses in parallel circuits and losses in the proximity between coil ends and iron casing. These are design issues which can be improved.

### ACKNOWLEDGMENTS

This work has been supported by public funding from the TEFT-program. The building and design was financed by Norpropeller AS in cooperation with Brunvoll AS. SmartMotor AS was responsible for the electrical machine design and assembly. This work has also been carried out in accordance with the project Energy Efficient All Electric Ship (AE3S). AE3S is a project with participants from NTNU (dept. of electric power engineering and dept. of marine technology), ABB, AkerKvaerner, Brunvoll, MARINTEK and Norpropeller.

### REFERENCES

- [1] Hanselman, D.C. "Brushless Permanent-Magnet Motor Design", McGraw-Hill Inc., 1994
- [2] Say, M.G., "Design of Alternating current Machines", Sir Isaac Pitman & Sons Ltd., 1948
- [3] Nilssen, R., Skaar, S.E., Lode, J., "Integrert propell og motor for elektrisk fremdrift av skip" Prosjektrapport, 2000, Department of Electrical Power Engineering, NTNU, Trondheim, Norway
- [4] [www.rolls-royce.com/marine](http://www.rolls-royce.com/marine)

## APPENDIX

TABLE II  
DIMENSIONS

Symbol	Quantity	Value
P	Power [kW]	100
U	Voltage [V]	400
n	Speed [rpm]	700
R <sub>ri</sub>	inner rotor yoke radius [mm]	300
R <sub>ro</sub>	outer rotor yoke radius [mm]	315
R <sub>mo</sub>	outer magnet radius [mm]	330
R <sub>si</sub>	inner stator radius [mm]	340
R <sub>sb</sub>	radius of slot [mm]	370
d <sub>r</sub>	thickness of rotor back iron [mm]	15
l <sub>m</sub>	length of magnet [mm]	15
g	effective air gap [mm]	10
d <sub>s</sub>	slot depth [mm]	30
τ <sub>p</sub>	pole pitch [mm]	94.2
ω <sub>m</sub>	magnet width [mm]	60
τ <sub>s</sub>	slotpitch [mm]	89.0
τ <sub>c</sub>	coil pitch [mm]	267
N <sub>s</sub>	number of slots	72
N <sub>p</sub>	number of poles	22
N <sub>c</sub>	number of coils	72

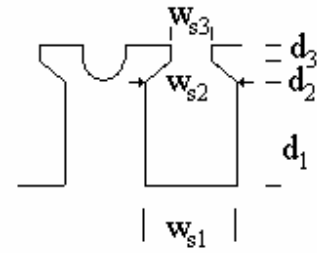


Fig 11, The slot geometry

TABLE III  
SLOT DIMENSIONS

Symbol	Value
$w_{s1}$	17 mm
$w_{s2}$	15 mm
$w_{s3}$	7.5 mm
$d_1$	23.5 mm
$d_2$	4.0 mm
$d_3$	2.5 mm
diso	0.3 mm

$$\begin{aligned}
 A_{slot} &= d_1 \cdot \frac{w_{s1} + w_{s2}}{2} + d_2 \cdot \frac{w_{s2} + w_{s3}}{2} \\
 A_{iso} &= d_{iso} \left( 2 \cdot d_1 + w_{s1} + 2 \cdot \sqrt{d_2^2 + w_{s3}^2} \right) \\
 A_{wedge} &= d_3 \cdot w_{s3}
 \end{aligned} \tag{18}$$